Vibronic coupling and band gap trends in CuGeO_{3} nanorods

Kenneth R. O'Neal, Amal al-Wahish, Zhaoqian Li, Peng Chen, Jae Wook Kim, Sang-Wook Cheong, Guy Dhalenne, Alexandre Revcolevschi, Xue-Tai Chen, and Janice L. Musfeldt

Phys. Rev. B **96**, 075437 — Published 28 August 2017

DOI: 10.1103/PhysRevB.96.075437

Vibronic coupling and band gap trends in $CuGeO_3$ nanorods

Kenneth R. O'Neal,[1] Amal al-Wahish,[1] Zhaoqian Li,[2] Peng Chen,[1] Jae Wook Kim,[3] Sang-Wook Cheong,[3] Guy Dhalenne,[4] Alexandre Revcolevschi,[4] Xue-Tai Chen,[5] and Janice L. Musfeldt[1,6]

[1]*Department of Chemistry, University of Tennessee, Knoxville, Tennessee 37996, USA*
[2]*Institute of Applied Technology, Hefei Institutes of Physical Science, Chinese Academy of Sciences, Hefei, Anhui 230031, PR China*
[3]*Rutgers Center for Emergent Materials and Department of Physics and Astronomy, Rutgers University, Piscataway, New Jersey 08854, USA*
[4]*SP2M-ICMMO UMR-CNRS 8182, Université Paris-Sud, 91405 Orsay Cedex, France*
[5]*State Key Laboratory of Coordination Chemistry, Nanjing National Laboratory of Microstructures, School of Chemistry and Chemical Engineering, Nanjing University, 210023, PR China*
[6]*Department of Physics and Astronomy, University of Tennessee, Knoxville, Tennessee 37996, USA*

(Dated: July 27, 2017)

We measured the optical response of $CuGeO_3$ nanorods in order to reveal size effects on the electronic properties. The vibronically-activated d-to-d color band excitations are activated by the 131 and 478 cm^{-1} phonons, with the relative contribution of the lower frequency O-Cu-O bending mode increasing with decreasing size until it dominates the process. We also uncover trends in the direct band gap, with the charge transfer transfer edge hardening with decreasing size. These findings advance the understanding of size effects in low-dimensional copper oxides.

I. INTRODUCTION

Charge-lattice coupling is one of the most fascinating and influential interactions in materials. It underpins numerous scientifically and technologically significant processes including superconductivity,[1–3] charge density wave transitions,[4–6] vibronic coupling,[7,8] and photochemical reactions.[9] One important example of vibronic coupling is the activation of d-manifold excitations in transition metal-containing materials.[10–13] This mechanism, in which an odd parity phonon interacts with an on-site d-to-d excitation to break inversion symmetry,[14,15] has been investigated in a number of bulk oxides including α-Fe_2O_3,[16] $CuGeO_3$,[17] and $BiFeO_3$.[18] Excitations of this type probe the crystal field environment and are colloquially called "color bands" when they appear in the visible range. They are thus responsible for the vivid colors of the aforementioned magnetic semiconductors. The mechanism is, however, relatively unexplored in nanomaterials.[19,20] The recent development of a suite of $CuGeO_3$ nanorods of different lengths[21] offers the opportunity to unravel size effects on the electronic properties - with special focus on vibronic coupling and band gap trends.

$CuGeO_3$ is well-known as the first inorganic spin-Peierls material.[22] This system consists of edge-sharing CuO_6 octahedra that form quasi-one-dimensional chains along the crystallographic c axis.[23,24] The Cu centers are d^9 and therefore S=1/2. The chains dimerize below the 14 K spin-Peierls transition,[22] and spin gaps open because singlets are formed.[22,25] This process is driven by spin-phonon interactions, and the coupling phonons have been identified as the 110 and 222 cm^{-1} Raman- and 295 cm^{-1} infrared-active B_{3u} modes.[26,27] The recent discovery of size-induced quenching of the spin-Peierls transition in $CuGeO_3$ nanorods[21] is also interesting from a mechanistic point of view. From the electronic point of view, $CuGeO_3$ is a semiconductor with 3.67 and 3.46 eV band gaps for $\vec{E} \parallel b$ and $\vec{E} \parallel c$, respectively.[17,28] Strong on-site d-to-d excitations activated by vibronic coupling appear below the gap and are responsible for the bright blue color of the crystals.[17] On the applications front, $CuGeO_3$ nanowires are already showing promise as modified electrode materials for cyclic voltammetry and as composite anode materials for high energy density lithium ion batteries.[29,30] A systematic study of the electronic properties will provide crucial support for these and other development efforts.

In this work, we reach beyond traditional temperature, magnetic field, and pressure tuning techniques to explore the optical properties of $CuGeO_3$ nanorods as a function of size. An additional and rather unique aspect of our approach is that while all nanorod diameters are similar, the growth habit is such that length can be controlled in the c direction.[21] Our spectroscopic measurements uncover several important electronic property trends in these materials including a crossover in the phonon that activates the d-to-d on-site excitations (from 478 $\rightarrow$ 131 cm^{-1}) and a charge gap that relaxes with ab-plane confinement and then hardens with decreasing rod length. As part of this effort, we test an updated vibronic coupling model against the behavior of on-site excitations in $CuGeO_3$ as well as several other oxides including α-Fe_2O_3 and Sr_3NiIrO_6.[31,32] This model includes a temperature-independent constant that emanates from distortion-, spin-orbit-, and exchange interaction-induced symmetry breaking. Taken together, these findings advance the understanding of size-driven changes in the optical properties of complex oxides. At the same time, they place these materials on a firm foundation for future device applications.

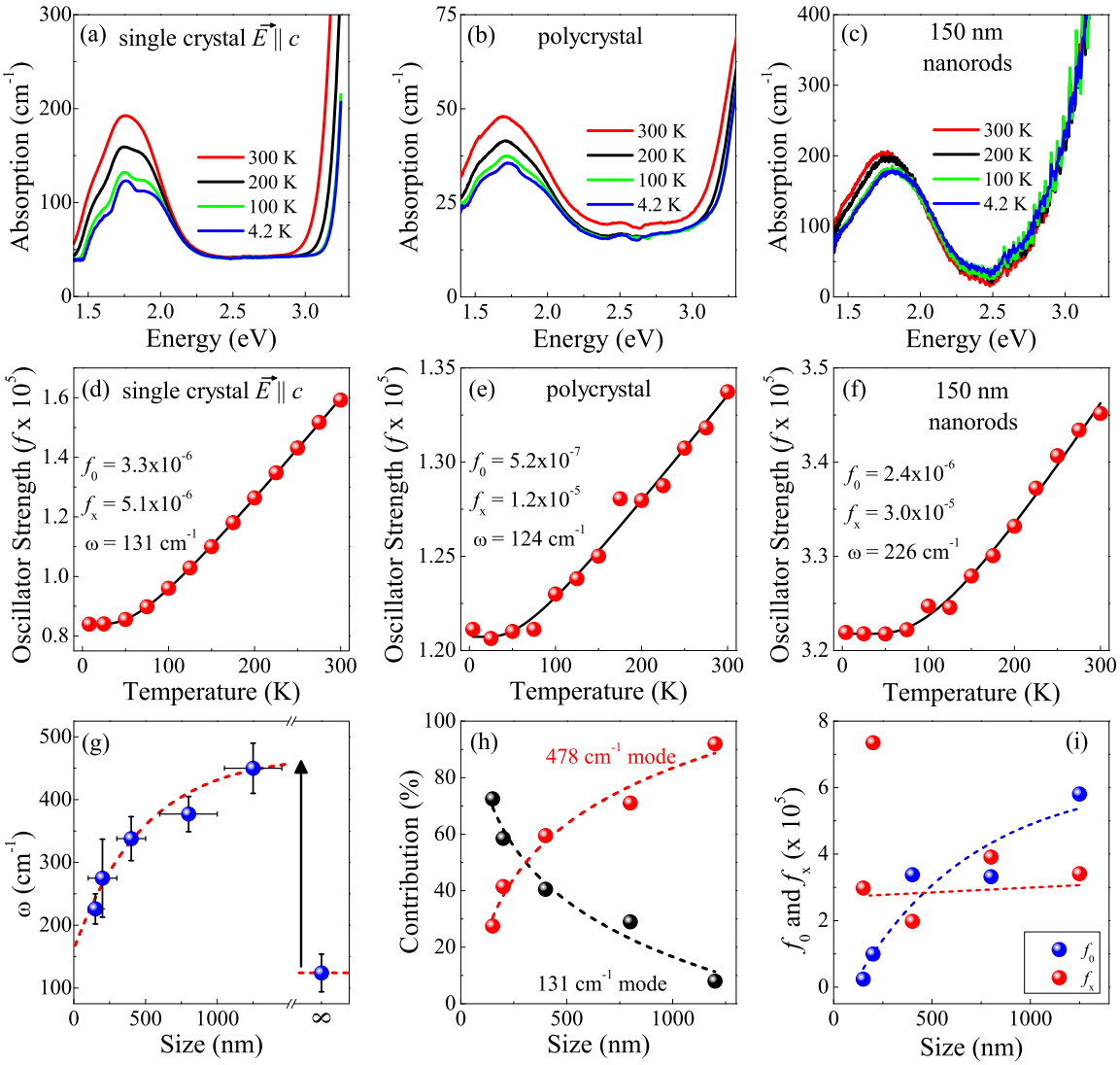

FIG. 1. Optical spectra of $CuGeO_3$ (a) single crystal, (b) polycrystal, and (c) nanorods at the indicated temperatures. (d-e) Oscillator strength of the color band for the above samples fit to the modified model discussed in the text, with the corresponding fit parameters indicated. (g) Frequency of the activating phonon (extracted from the modified model for each sample measured) as a function of size. (h) Percent contribution to the weighted average of the two participating phonons. The dashed lines guide the eye. (i) f_0 and f_x as determined for the $CuGeO_3$ nanorods.

II. METHODS

$CuGeO_3$ nanorods were prepared by hydrothermal methods as described previously[21] and characterized using scanning electron microscopy, susceptibility, and x-ray diffraction.[33] For comparison, single and polycrystalline samples were made by floating zone techniques using an image furnace.[34] Powdered nanorod and polycrystal samples were mixed with a transparent KBr matrix to form pressed pellets, whereas the single crystal was cleaved in the bc-plane to an appropriate optical density of $\approx 40\mu$m. Optical spectra were collected using a Perkin Elmer Lambda-900 (0.4-6.8 eV). Absorption was calculated as $\alpha = \frac{-1}{hd} ln(T(\omega))$, where h is sample loading, d is thickness, and $T(\omega)$ is measured transmittance. Temperature control was achieved with an open flow helium cryostat (4.2-300 K). Oscillator strength was calculated as $f = \frac{2mc\epsilon_0 c}{N\pi e^2} \int_{\omega 1}^{\omega 2} n\alpha(\omega) d\omega$, where N is the density of Cu centers, $n \approx 2.5$ is the refractive index, e and m are the charge and mass of an electron, ϵ_0 is the vacuum dielectric constant, c is the speed of light, and ω_1 and ω_2 are the frequency limits of integration.[17,35] Proper backgrounds were subtracted before integration to isolate the oscillator strength of the d-to-d excitations.

III. RESULTS AND DISCUSSION

III.1. Size effects on the electronic properties of $CuGeO_3$ nanorods

Figure 1 (a-c) displays representative optical spectra of single crystalline, polycrystalline, and 150 nm nanorods of $CuGeO_3$.[36] There are two main structures of interest. The band near 1.75 eV is assigned as a set of vibronically-allowed on-site d-to-d excitations of Cu^{2+}.[17] These excitations are activated by coupling with an odd-parity phonon and responsible for the bright blue color of $CuGeO_3$.[17] The sharply rising absorption above 3 eV is assigned as the edge of the direct gap. The latter is

charge transfer in nature.[17] Both structures are common in semiconducting transition metal oxides.[11,37–39]

The oscillator strength of the d-to-d excitations is strongly temperature-dependent [Fig. 1 (d-f)], characteristic of the phonon-assisted activation mechanism.[40] This process is typically modeled as $f = f_0 \coth(\frac{\hbar\omega}{2k_BT})$, where ω is the frequency of the activating phonon, f_0 is the limiting low temperature value of the oscillator strength, T is temperature, and h and k_B have their usual values. In prior work on $CuGeO_3$ single crystals, this model was used to quantify temperature-induced changes in the oscillator strength of the d-to-d excitations. A coupled phonon frequency of $\omega \approx 250$ cm^{-1} was extracted.[17]

Interestingly, this model does not agree well with our newly measured single crystal spectra, particularly in the low and high temperature regions where we have many more data points than in the prior work. Inclusion of a temperature-independent constant, $f = f_x + f_0 \coth(\frac{\hbar\omega}{2k_BT})$, provides a better fit over the full temperature range. While the revised model improves the fit, it also impacts the coupled phonon frequency, ω. Applying the extended model to our single crystal data, we find $\omega = 131$ cm^{-1}. Both models yield values that are within the range of observed phonons in $CuGeO_3$, but the result of the modified fit (131 cm^{-1}) correlates directly with an a-polarized B_{1u} phonon whereas the result of the original model (250 cm^{-1}) does not match well with any phonon.[41] We discuss the physical significance of the additive constant f_x below.

We now turn to the size-dependent electronic properties of the $CuGeO_3$ nanorods. Importantly, the extended model incorporating f_x is required to produce a reasonable fit to any of the nanorod data sets (see Supplemental Information). We therefore apply the revised model to the nanorod data in order to reveal size effects on the vibronic coupling in $CuGeO_3$. As an example, the optical response of the 150 nm nanorods is shown in Fig. 1 (c). A fit of the oscillator strength as a function of temperature yields a coupling phonon frequency of 226 cm^{-1}. This value is quite different from that of the single crystal.

Figure 1 (g) displays the coupling phonon frequency ω extracted from this analysis as a function of size. There is a large jump from the polycrystal value and a strong size dependence within the nanorods. Importantly, the shifts are far too large to correlate with a single phonon mode. In cases where more than one phonon activates the excitation, ω represents a weighted average of the participating phonon frequencies.[42] Extrapolation of the nanorod trend reveals endpoints of 131 and 478 cm^{-1}, which correspond precisely to the B_{1u} O-Cu-O bending and O-Cu-O asymmetric stretching modes, respectively.[41] Comparing these frequencies with the value of ω from the fitting, we can back-calculate the contribution of each of the aforementioned modes to the activation of the d-to-d excitations as function of nanorod length [Fig. 1 (h)]. Doing so reveals a clear crossover in the activating phonon. We find that the Cu^{2+} on-site excitations in long nanorods are mostly activated by the 478 cm^{-1} mode. The 131 cm^{-1} mode begins to play a role as length decreases, eventually becoming the dominant coupling phonon in the shortest rods. We note that a similar size-induced crossover of the activating phonon takes place in α-Fe_2O_3 nanoparticles.[19] Whether this is a general aspect of vibronic coupling in nanoscale transition metal oxides remains to be tested in other systems.

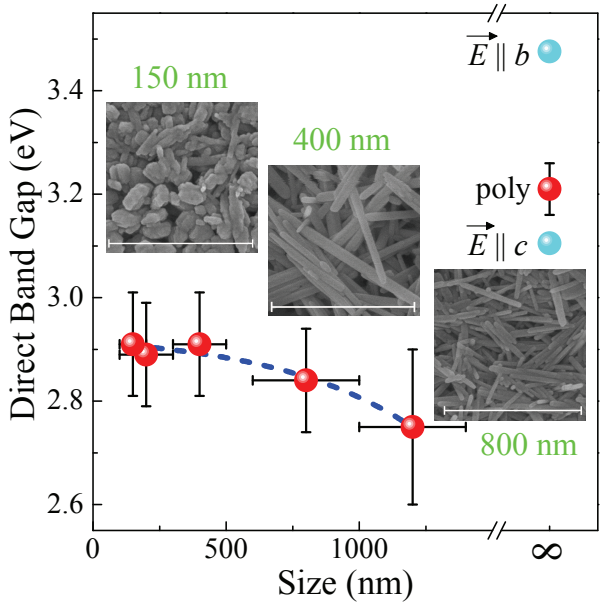

FIG. 2. Size dependence of the $CuGeO_3$ optical band gap as determined by the charge transfer edge. Scanning electron microscope images of representative nanorods are included where the scale bars is 500 nm for the 150 nm rods, and 1000 nm for the larger sizes.

The optical properties of this set of nanomaterials also allow exploration of the charge transfer edge, which defines the direct band gap in $CuGeO_3$. It is obtained from plots of $(\alpha \cdot E)^2$ vs. energy extrapolated to the abscissa. Figure 2 summarizes the size dependence of this structure. There are two important trends. First, the charge gap redshifts by 0.5 eV between the polycrystal and the longest nanorods. This is different than the standard size-induced band gap hardening[43–46] and can likely be attributed to aspect ratio effects and the rod-like morphology. Second, the charge gap hardens with decreasing size - from 2.7 eV in the longest nanorods to 2.9 eV in the shortest. This blue shift is overall consistent with modeling and experiments on a number of other materials,[46–49] and in this case, the trend may also be due to development of flatter bands from reduced intralayer bonding.[50] We anticipate much more rapid band gap hardening at even smaller sizes,[44,51,52] a supposition that can be tested as smaller $CuGeO_3$-based nanomaterials become available.

III.2. Extended oscillator strength analysis: the role of f_x

As mentioned above, we include a temperature-independent constant f_x in the extended oscillator strength model. As exemplified by the r^2 values [Fig. 3 (a,b)], this improves the overall fit to the single crystal data. The difference between the two models is subtle, and it might not have been noticed without many low and high temperature data points and a careful fitting analysis. This modification is, however, crucial for reasonable fitting of the nanorod data [Fig. 3 (c,d)]. Fits to the standard vibronic coupling model for the 150 nm rods are, for instance, wholly unacceptable (r^2=0.87). The addition of f_x improves the r^2 value to 0.99 - in the acceptable range.

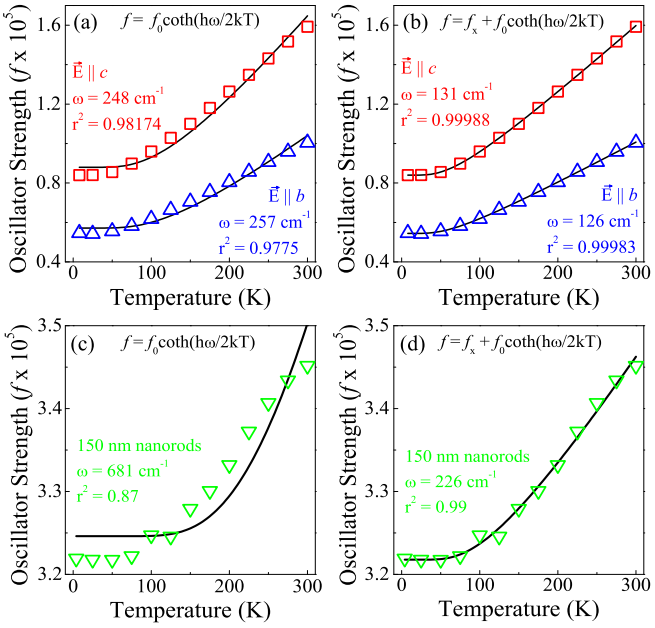

FIG. 3. Oscillator strength analysis for d-to-d excitations measured along the the b and c directions of single crystalline $CuGeO_3$ using (a) the standard model and (b) the modified model. The same comparison between standard (c) and updated (d) models for the smallest nanorods emphasizing the necessity of the f_x parameter.

For the extended vibronic coupling model to have a firm foundation beyond simply improving the fits, the additional term must have some physical origin. There are many cases where the basic model has been successfully applied.[17,53–58] A literature search also reveals that a constant like f_x has been included in modeling efforts for a number of other materials. For example, in $KCuF_3$ this term is ascribed to magnetic dipole-allowed transitions.[59] However, the authors show that these features are small and temperature-dependent, in contrast with the model and large value of f_x. In $CsFeCl_3$, a constant the same order of magnitude as f_0 was included, although the physical origin was not discussed at all.[60] A study of Ag^+ ions in various halide crystals even found f_x to be negative.[61] This term is clearly not well-understood and requires further investigation.

In order to gain insight into the origin of f_x, we examined d-to-d excitations in several other bulk oxides including α-Fe_2O_3 and Sr_3NiIrO_6 (Supplemental Information). Again, the extended model yields reasonable fits to the oscillator strength trends. The results reveal that f_x can be smaller or larger than f_0 as in α-Fe_2O_3 and Sr_3NiIrO_6, respectively. Based on these examples, f_x likely represents oscillator strength contributed by symmetry-breaking processes such as spin-orbit coupling, exchange interactions, or distorted crystal field environment, which vary from material to material - as does f_x. This is why the term is present even in single crystal samples.

Returning to $CuGeO_3$, the size dependence of f_x [Fig. 1 (i)] may also hold some clue as to its origin. The value is small for both polarizations of the single crystal ($\approx 4 \times 10^{-6}$), but larger and nearly constant for the nanorods ($\approx 4 \times 10^{-5}$, excluding the 200 nm rods). The increase in f_x on progressing from single crystal to nanorod morphology likely springs from additional distortion and broken symmetry at the grain boundaries. We therefore expect f_x to increase sharply at even smaller sizes as the surface-to-volume ratio rises.

IV. CONCLUSION

We measured the optical properties of a suite of $CuGeO_3$ nanorods and compared the response with single and polycrystal samples in order to explore size effects on the electronic properties. By so doing, we reveal a size-dependent crossover in the phonon that activates the Cu^{2+} on-site excitations (from 478 $\rightarrow$ 131 cm^{-1}). The latter dominates at small sizes. As part of this analysis, we test an extended model for vibronic coupling and argue that the expression should also contain a distortion term. The latter is present but challenging to detect in single crystals. This term becomes very important in the nanorods - probably due to additional symmetry-breaking distortions at the surface. Band gap trends involve substantial size-dependent shifts in the charge transfer edge. The direct gap redshifts upon formation of the nanorods and subsequently hardens to 2.9 eV in the smallest nano-materials measured here. These findings highlight the importance of size effects in determining the electronic properties of multifunctional materials.

V. ACKNOWLEDGMENTS

Research on $CuGeO_3$ and α-Fe_2O_3 at the University of Tennessee is supported by the Materials Science Division, Office of Basic Energy Sciences, U.S. Department of Energy under Award DE-FG02-01ER45885. Work on Sr_3NiIrO_6 is funded by the National Science Foundation DMREF program (DMR-1629079). Crystal growth at

Rutgers (α-Fe_2O_3 and Sr_3NiIrO_6) is supported by the National Science Foundation DMREF program (DMR-1629059). We thank Lei Chen and Ziling Xue for useful discussions.

VI. SUPPORTING INFORMATION

Supporting information is available including structural characterization and oscillator strength trends for $CuGeO_3$ polycrystal and all nanorod samples as well as single crystalline α-Fe_2O_3 and Sr_3NiIrO_6.

[1] A. Bhaumik, R. Sachan, and J. Narayan. ACS Nano **11**, 5351 (2017).

[2] T. Bi, D. P. Miller, A. Shamp, and E. Zurek. Angew. Chemie Int. Ed. 1–5 (2017).

[3] C. Zhang, Z. Liu, Z. Chen, Y. Xie, R. He, S. Tang, J. He, W. Li, T. Jia, S. N. Rebec, E. Y. Ma, H. Yan, M. Hashimoto, D. Lu, S.-K. Mo, Y. Hikita, R. G. Moore, H. Y. Hwang, D. Lee, and Z. Shen. Nat. Commun. **8**, 14468 (2017).

[4] S. Yan, D. Iaia, E. Morosan, E. Fradkin, P. Abbamonte, and V. Madhavan. Phys. Rev. Lett. **118**, 106405 (2017).

[5] D. Mou, A. Sapkota, H.-H. Kung, V. Krapivin, Y. Wu, A. Kreyssig, X. Zhou, A. I. Goldman, G. Blumberg, R. Flint, and A. Kaminski. Phys. Rev. Lett. **116**, 196401 (2016).

[6] E. Navarro-Moratalla, J. O. Island, S. Mañas Valero, E. Pinilla-Cienfuegos, A. Castellanos-Gomez, J. Quereda, G. Rubio-Bollinger, L. Chirolli, J. A. Silva-Guillén, N. Agraït, G. A. Steele, F. Guinea, H. S. J. van der Zant, and E. Coronado. Nat. Commun. **7**, 11043 (2016).

[7] Y. Ma, P. Skytt, N. Wassdahl, P. Glans, D. C. Mancini, J. Guo, and J. Nordgren. Phys. Rev. Lett. **71**, 3725 (1993).

[8] F. A. Balmer, S. Kopec, H. Köppel, and S. Leutwyler. J. Phys. Chem. A **121**, 73 (2017).

[9] R. G. McKinlay, J. M. Żurek, and M. J. Paterson. Adv. Inorg. Chem. **62**, 351 (2010).

[10] W. S. Choi, K. Taniguchi, S. J. Moon, S. S. A. Seo, T. Arima, H. Hoang, I.-S. S. Yang, T. W. Noh, and Y. S. Lee. Phys. Rev. **81**, 205111 (2010).

[11] M. M. Waegele, H. Q. Doan, and T. Cuk. J. Phys. Chem. C **118**, 3426 (2014).

[12] H. J. Park, C. H. Sohn, D. W. Jeong, G. Cao, K. W. Kim, S. J. Moon, H. Jin, D.-Y. Cho, and T. W. Noh. Phys. Rev. B **89**, 155115 (2014).

[13] H. Nishihara, A. Furuhashi, N. Yamaguchi, R. Koborinai, and T. Katsufuji. Phys. Rev. B **92**, 140401(R) (2015).

[14] D. D. Sell, R. L. Greene, and R. M. White. Phys. Rev. **158**, 489 (1967).

[15] L. L. Lohr Jr. Coord. Chem. Rev. **8**, 241 (1972).

[16] L. A. Marusak, R. Messier, and W. B. White. J. Phys. Chem. Solids **41**, 981 (1980).

[17] M. Bassi, P. Camagni, R. Rolli, G. Samoggia, F. Parmigiani, G. Dhalenne, and A. Revcolevschi. Phys. Rev. B **54**, R11030 (1996).

[18] X. S. Xu, T. V. Brinzari, S. Lee, Y. H. Chu, L. W. Martin, A. Kumar, S. McGill, R. C. Rai, R. Ramesh, V. Gopalan, S. W. Cheong, and J. L. Musfeldt. Phys. Rev. B **79**, 134425 (2009).

[19] K. R. O'Neal, J. M. Patete, P. Chen, B. S. Holinsworth, J. M. Smith, N. Lee, S.-W. Cheong, S. S. Wong, C. Marques, M. C. Aronson, and J. L. Musfeldt. J. Chem. Phys. **141**, 044710 (2014).

[20] Z. Cui, C. Xie, X. Feng, N. Becknell, P. Yang, Y. Lu, X. Zhai, X. Liu, W. Yang, Y.-D. Chuang, and J. Guo. J. Phys. Chem. Lett. **8**, 319 (2017).

[21] Z.-Q. Li, L. Zhang, Y. Song, X.-T. Chen, J. L. Musfeldt, and Z.-L. Xue. CrystEngComm **16**, 850 (2014).

[22] M. Hase, I. Terasaki, and K. Uchinokura. Phys. Rev. Lett. **70**, 3651 (1993).

[23] H. Völlenkle, A. Wittmann, and H. Nowotny. Monatsh Chem **02**, 1353 (1967).

[24] M. Braden, G. Wilkendorf, J. Lorenzana, M. Aín, G. J. McIntyre, M. Behruzi, G. Heger, G. Dhalenne, and A. Revcolevschi. Phys. Rev. B **54**, 1105 (1996).

[25] T. M. Brill, J. P. Boucher, J. Voiron, G. Dhalenne, A. Revcolevschi, and J. P. Renard. Phys. Rev. Lett. **73**, 1545 (1994).

[26] M. Braden, B. Hennion, W. Reichardt, G. Dhalenne, and A. Revcolevschi. Phys. Rev. Lett. **80**, 3634 (1998).

[27] J. L. Musfeldt, Y. J. Wang, S. Jandl, M. Poirier, A. Revcolevschi, and G. Dhalenne. Phys. Rev. B **54**, 469 (1996).

[28] D. Benea, V. Pop, and O. Isnard. Phys. Rev. B **55**, 13528 (2008).

[29] L. Z. Pei, Y. K. Xie, Y. Q. Pei, Z. Y. Cai, and C. G. Fan. J. Nanotechnol. Eng. Med. **4**, 031003 (2013).

[30] Z. Chen, Y. Yan, S. Xin, W. Li, J. Qu, Y. G. Guo, and W. G. Song. J. Mater. Chem. A **1**, 11404 (2013).

[31] P. Chen, O. Günaydın-Şen, W. J. Ren, Z. Qin, T. V. Brinzari, S. McGill, S.-W. Cheong, and J. L. Musfeldt. Phys. Rev. B **86**, 014407 (2012).

[32] E. Lefrançois, A. M. Pradipto, M. Moretti Sala, L. C. Chapon, V. Simonet, S. Picozzi, P. Lejay, S. Petit, and R. Ballou. Phys. Rev. B **93**, 224401 (2016).

[33] See the Supporting Information for details.

[34] A. Revcolevschi and G. Dhalenne. Adv. Mater. **5**, 657 (1993).

[35] C. J. Ballhausen. *Introduction to ligand field thoery.* McGraw-Hill, New York (1962).

[36] Note that the difference in absorption levels is likely due to error in sample thickness and loading.

[37] B. Fromme, M. Möller, C. Bethke, U. Brunokowski, and E. Kisker. Phys. Rev. B **57**, 12069 (1998).

[38] R. K. Kawar, P. S. Chigare, and P. S. Patil. Appl. Surf. Sci. **206**, 90 (2003).

[39] C. F. Hague, J.-M. Mariot, V. Ilakovac, R. Delaunay, M. Marsi, M. Sacchi, J.-P. Rueff, and W. Felsch. Phys. Rev. B **77**, 045132 (2008).

[40] O. G. Holmes and D. S. McClure. J. Chem. Phys. **26**, 1686 (1957).

[41] Z. V. Popović, S. D. Dević, V. N. Popov, G. Dhalenne, and A. Revcolevschi. Phys. Rev. B **52**, 4185 (1995).

[42] C. D. Flint. Coord. Chem. Rev. **14**, 47 (1974).

[43] C. S. Biju, D. H. Raja, and D. P. Padiyan. Chem. Phys. Lett. **610-611**, 103 (2014).

[44] S. Kan, T. Mokari, E. Rothenberg, and U. Banin. Nat. Mater. **2**, 155 (2003).
[45] L. M. Kukreja, S. Barik, and P. Misra. J. Cryst. Growth **268**, 531 (2004).
[46] S. Sarkar and K. Chattopadhyay. Physica E **44**, 1742 (2012).
[47] L. E. Brus. J. Chem. Phys. **80**, 4403 (1984).
[48] E. Cho, H. Jang, J. Lee, and E. Jang. Nanotechnology **24**, 215201 (2013).
[49] B. Wei, K. Zheng, Y. Ji, Y. Zhang, Z. Zhang, and X. Han. Nano Lett. **12**, 4595 (2012).
[50] K. R. O'Neal, A. al-Wahish, Z. Li, G. Dhalenne, A. Revcolevschi, X.-T. Chen, and J. L. Musfeldt. In preparation.
[51] I. Moreels, K. Lambert, D. Smeets, D. D. Muynck, T. Nollet, J. C. Martins, F. Vanhaecke, A. Vantomme, C. Delerue, G. Allan, and Z. Hens. ACS Nano **3**, 3023 (2009).
[52] N. Satoh, T. Nakashima, K. Kamikura, and K. Yamamoto. Nat. Nanotechnol. **3**, 106 (2008).
[53] J. Brynestad, H. L. Yakel, and G. P. Smith. J. Chem. Phys. **45**, 4652 (1966).
[54] H. Ohkura and J. Yagi. J. Phys. Soc. Japan **24**, 653 (1968).
[55] K. Fussgaenger. Phys. Status Solidi **36**, 645 (1969).
[56] J. R. Dickinson and K. E. Johnson. J. Mol. Spectrosc. **33**, 414 (1970).
[57] A. J. McCaffery, J. R. Dickson, and P. N. Schatz. Inorg. Chem. **9**, 1563 (1970).
[58] J. D. Lebedda and R. A. Palmer. Inorg. Chem. **11**, 484 (1972).
[59] J. Deisenhofer, I. Leonov, M. V. Eremin, C. Kant, P. Ghigna, F. Mayr, V. V. Iglamov, V. I. Anisimov, and D. van Der Marel. Phys. Rev. Lett. **101**, 157406 (2008).
[60] T. Tsuboi, M. Chiba, and Y. Ajiro. Phys. Rev. B **32**, 354 (1985).
[61] K. Fussgaenger, W. Martienssen, and H. Bilz. Phys. Status Solidi **12**, 383 (1965).